A static optimization approach to vehicle energy management of a hybrid electric vehicle with engine start/stop

Trevino Rojas, R.

Award date:
2020

THESIS REPORT:
A STATIC OPTIMIZATION APPROACH TO VEHICLE ENERGY MANAGEMENT OF A HYBRID ELECTRIC VEHICLE WITH ENGINE START/STOP

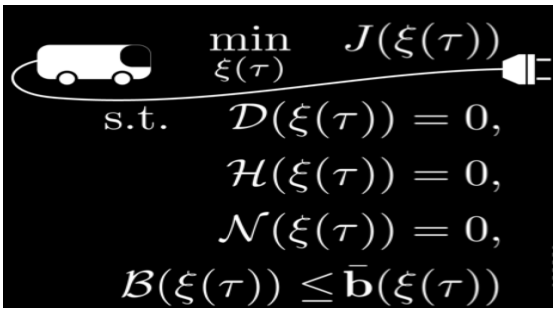

Master: Systems and Control
Department: Electrical Engineering
Research Group: Control Systems

Student: Roberto Treviño Rojas
e-mail: r.trevino.rojas@student.tue.nl
IDNR: 1298690

Thesis Supervisor: M.C.F. Donkers
e-mail: m.c.f.donkers@tue.nl

Date of presentation: 27 of October 2020

TU/e Technische Universiteit Eindhoven University of Technology

Declaration concerning the TU/e Code of Scientific Conduct for the Master's thesis

I have read the TU/e Code of Scientific Conduct[i].

I hereby declare that my Master's thesis has been carried out in accordance with the rules of the TU/e Code of Scientific Conduct

Date

28 of October 2020

Name

Roberto Treviño Rojas

ID-number

1298690

Signature

Roberto Treviño

Submit the signed declaration to the student administration of your department.

[i] See: http://www.tue.nl/en/university/about-the-university/integrity/scientific-integrity/
The Netherlands Code of Conduct for Academic Practice of the VSNU can be found here also.
More information about scientific integrity is published on the websites of TU/e and VSNU

January 15 2016

A Static Optimization Approach to Vehicle Energy Management of a Hybrid Electric Vehicle with Engine Start/Stop

Roberto Treviño Rojas
ID: 1298690 | e-mail: r.trevino.rojas@student.tue.nl

***Abstract*— This thesis presents a solution to the Vehicle Energy Management (VEM) problem for a case study of a hybrid electric heavy duty truck with engine start/stop. Here, a power and torque based modeling framework is used to describe the behaviour of the subsystems to be included in a VEM Optimal Control Problem (OCP). This OCP is recasted as a mixed-integer non-linear nonconvex static optimization problem. Three approaches are presented in order to handle the integer decision variable representing the engine start/stop. Moreover, each approach is simulated over two different standardized velocity profiles. Numerical results of the simulations show advantages in terms of obtained solution and minimization time between the three approaches.**

I. INTRODUCTION

Given the increasing emissions of carbon dioxide (CO_2), i.e., 1 gigatonne per year from 2000 to 2010 according to [1], many measures in order to mitigate these emissions have been implemented, going from legislations to enforce fuel economy improvement to integration and deployment of fully electrical vehicles (EV) and hybrid electric vehicles (HEV). In this report, we focus on the latter, which is of special interest given that it involves challenging problems of its own that are not touched upon in cases of only combustion engine and fully electric vehicles.

Within an HEV, the power demand in order to move the vehicle is split among the different powertrain energy sources in order to operate the internal combustion engine (ICE) as efficiently as possible. Algorithms developed for finding the best power split are known as vehicle energy management strategies (VEM), which in its most general form can be formulated as a constrained optimal control problem (OCP). Three widely used methods for solving these optimal control problems can be classified into: dynamic programming (DP), indirect, and direct methods.

The DP approach is based on the principle of optimality [2], where both continuous and discrete variables are quantized, e.g., torque and gears, respectively. Then the resulting discrete static optimization problem is solved to determine the solution of the VEM problem [3], [4], [5] and [6]. The main drawback of this method is the so called 'curse of dimentionality', which comes from the computational expensiveness of gridding the entire state space which depends on the number of components. In the group of indirect methods, Pontryagin minimum principle (PMP) is applied to obtain the optimality conditions and reduce the original problem to an equivalent boundary value problem (BVP) [7], which in the presence of state constraint is hard to solve [8], [9]. In the direct methods group, the time is quantized in order to obtain a finite-time problem [10], [11], [12], where multi-state with both input and state constraints can be applied but in the presence of both continuous and discrete variables result in large-scale mixed-integer problems.

Several researchers have addressed this large-scale mixed-integer problem differently. In [13], an objective function representing the fuel consumption depending in both continuous and discrete variables is presented. Then, the discrete variable is assumed to be fixed (known trajectory) making the minimization problem only depend on the continuous variable. This objective function is evaluated several times while taking a different value of the discrete variable each time, and afterwards, the minimum of the result of each minimization is taken. Furthermore in [14], a predictive Eco-driving Advice is presented, where the original problem depends in both discrete and continuous variables. Here, the discrete variable is relaxed in order to obtain a problem depending only on continuous variables, then the solution of the discrete variable is recovered by a special rounding technique. Similarly, in [15] the gear ratios in the gearbox of the vehicle are relaxed from integers to continuous variables, this in order to simplify the original problem from mixed-integer to only contain continuous variables. Additionally, an energy optimal intersection problem is shown in [16], where the original OCP depends again on discrete and continuous variables. Here the original problem is successively approximated by quadratic functions while maintaining binary variables, and is solved with a dedicated solver capable of handling continuous

and discrete variables.

The aforementioned strategies have been implemented in their own specific applications, however, several open questions regarding these methodologies exist. For instance, how fast does each strategy work and what are the numerical results of applying them onto the same VEM case study. Therefore, in this work we present an OCP which aims to minimize the fuel consumption of a HEV for a standardized trajectory while including state and input constraints and a switching binary variable representing the start/stop behaviour of the combustion engine.

The remainder of this report is organized as follows. In section II the case study is introduced, where the modeling of the subsystems and the problem formulation of the OCP is presented as a Mixed-Integer Non-linear Problem (MINLP). Section III proposes three solution methods for the VEM problem, followed by simulation results of each approach in Section IV. At last, Section V presents conclusions and perspectives on possible future work.

II. Case study

In this section, the topology of the HEV is introduced, followed by the mathematical description of the subsystems acting in the case study network. Then, the formulation of the discrete-time OCP is presented, which turn out to be a non-convex mixed-integer nonlinear program.

A. Case study VEM and topology

The objective in the Vehicle Energy Management of this project is to minimize the cumulative fuel consumption, i.e.,

$$\min \sum_{k \in \mathscr{K}} m_{f,k}, \tag{1}$$

where $m_{f,k}$ is the fuel consumption rate at instance k for all times $k \in \mathscr{K}$, where $\mathscr{K} = \{0,1,...,K-1\}$ and K is the length of the given velocity profile. This fuel consumption rate has to be minimized while being bounded by all the constraints and subsystems acting in the vehicle. An overview of the topology considered in this work, the subsystems models and constraints will be developed below.

In Figure 1 the topology under consideration for the case study can be depicted. The vehicle network includes an internal combustion engine (ICE), an electric machine (EM), a high voltage battery (HVB) and mechanical friction brakes (BR). The torque the ICE, EM and BR can provide are represented by u_{ice}, u_{em} and u_{br}, respectively. The energy stored in the battery and the power it can

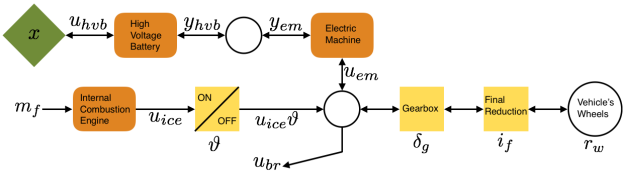

Fig. 1: Topology of case study HEV.

deliver are represented by x and u_{hvb}. Furthermore, the selected gear, final reduction and vehicle's wheels radius are δ_g, i_f and r_w, respectively. For clarity and ease of notation, the sub-index denoting the time dependency k has been dropped in the figure.

B. Fuel consumption model

As mentioned previously, the goal of this work is to minimize the fuel consumption rate (1). Several fuel consumption rate models have been studied and compared in [17], in this work we consider a polynomial model where the control input is the engine torque ($u_{ice,k}$) and has the form of:

$$m_{f,k} = \alpha_1 \omega_{ice,k} + \alpha_2 \omega_{ice,k}^2 + \alpha_3 \omega_{ice,k} u_{ice,k}, \tag{2}$$

where α_i, $i \in \{1,2,3\}$ are polynomial coefficients identified from experimental data sets through least squares fitting problem as:

$$\min_{\Psi_{ice}} ||e_{ice}||_2^2 = ||M_f - W_{ice}\Psi_{ice}||_2^2, \tag{3}$$

where Ψ_{ice} corresponds to the polynomial coefficients as:

$$\Psi_{ice} = [\alpha_1, \alpha_2, \alpha_3]^\top, \tag{4}$$

and M_f and W_{ice} are the evolution of the fuel consumption and angular speed and torque supplied by ICE, respectively:

$$M_f = \begin{bmatrix} m_{f,1} \\ m_{f,2} \\ \vdots \\ m_{f,N} \end{bmatrix}, \quad W_{ice} = \begin{bmatrix} \omega_{ice,1} & \omega_{ice,1}^2 & \omega_{ice,1}u_{ice,1} \\ \omega_{ice,2} & \omega_{ice,2}^2 & \omega_{ice,2}u_{ice,2} \\ \vdots & \vdots & \vdots \\ \omega_{ice,N} & \omega_{ice,N}^2 & \omega_{ice,N}u_{ice,N} \end{bmatrix}. \tag{5}$$

The corresponding values of (4) and the mean squared error can be found in Table I.

C. Vehicle dynamics

A hybrid electric vehicle compared with a purely internal combustion engine vehicle, is characterized by two or more movers and power sources. A motivation for developing HEVs is the possibility to combine the

TABLE I: HEV parameters

Variable	Value	Definition	Units
g	9.81	gravitational acceleration	$[\frac{m}{s^2}]$
m_{veh}	15000	vehicle's mass	[kg]
i_f	2.71	final reduction	[-]
r_w	0.5512	wheels radius	[m]
ρ_{air}	1.225	air density	$[\frac{kg}{m^3}]$
A_f	7.54	Vehicle frontal area	$[m^2]$
c_d	0.7	vehicle's drag coefficient	[-]
c_r	6.4×10^{-3}	tires rolling coefficient	[-]
$c_{ine,1}$	1.04	Inertia coefficient	[-]
$c_{ine,2}$	0.0025	Inertia coefficient	[-]
R	0.333	Series resistance	[Ohm]
U_{oc}	660	Open circuit voltage	$[V]$
$\overline{x}$	6.3	max HVB energy	[kWh]
$\underline{x}$	0.63	min HVB energy	[kWh]
$\overline{u}_{hvb}$	154	max HVB power	[kW]
$\underline{u}_{hvb}$	-114	min HVB power	[kW]
γ_3	0.0562	y_{em} coefficient	$[\frac{W}{(N.m)^2}]$
γ_2	1.012	y_{em} coefficient	$[\frac{W.s}{rad.N.m}]$
γ_1	0.1789	y_{em} coefficient	$[\frac{W.s}{rad}]$
e_{em}	9.602×10^{-3}	y_{em} norm error	[W]
$\overline{u}_{em}$	1041	max torque	[N.m]
$\underline{u}_{em}$	-1041	min torque	[N.m]
α_1	0.0153	m_f coefficient	$[\frac{gr}{rad}]$
α_2	-5.232×10^{-5}	m_f coefficient	$[\frac{gr}{rad^2}]$
α_3	4.918×10^{-5}	m_f coefficient	$[\frac{gr}{rad.N.m}]$
e_{ice}	1.0636×10^{-3}	norm error	[gr]
$\overline{u}_{ice}$	2900	max torque	[N.m]
$\underline{u}_{ice}$	0	min torque	[N.m]

advantage points of combustion engines and electric vehicles.

The longitudinal vehicle dynamics of the vehicle is given by:

$$I_{veh,k} \frac{v_{veh,k+1} - v_{veh,k}}{\Delta_t} = F_{w,k} - F_{br,k} - F_{r,k} - F_{d,k} \quad (6)$$

where Δ_t represents the discretization time steps as $\Delta_t = \frac{t_f - t_0}{K}$ for some $K \in \mathbb{N}$, $I_{veh,k}$ is the vehicle's inertia, $v_{veh,k}$ is the vehicle's velocity, $F_{w,k}$ is the propulsion force at the wheels, $F_{br,k}$ is the braking force, $F_{r,k}$ is the rolling resistance experienced by the tires and $F_{d,k}$ is the aerodynamic drag, all of them at time instance k.

Figure 2 show the two standard driving cycles considered in this work, from which, the vehicle inertia, acceleration, resistance forces, selected gear and angular speed are obtained and known for all times. The vehicle inertia and resistance forces are given by:

$$I_{veh,k} = m_{veh}(c_{ine,1} + c_{ine,2}(\delta_{g,k} i_f)^2) \quad (7)$$

$$F_{d,k} = \tfrac{1}{2} \rho_{air} c_d A_f v_{veh,k}^2, \quad (8)$$

$$F_{r,k} = c_r m_{veh} g \cos(\theta), \quad (9)$$

where m_{veh} is the vehicles mass, $\delta_{g,k}$ is the selected gear ratio, i_f the final ratio, ρ_{air} represents the air density, c_d the drag coefficient, A_f the frontal area of the vehicle, c_r the rolling friction coefficient, g the gravitational acceleration and θ the road slope. The gear selection is done through a set of rules presented in Appendix I, where the velocity of the vehicle is compared to a predefined set of velocities which indicate the moment where the vehicle should either shift up or down. The predefined set of velocities varies depending whether the vehicle's acceleration is positive, negative or zero. Furthermore, the angular speed of the engine directly depends on the selected gear and the vehicle's velocity as:

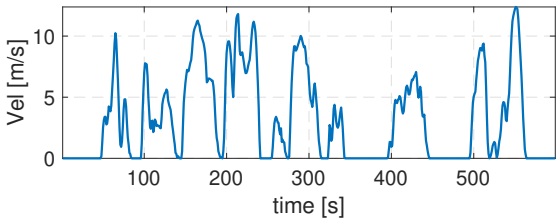

(a) New York City Cycle (NYCC) velocity profile.

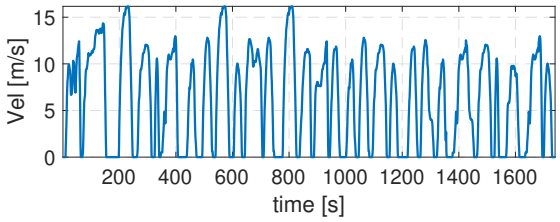

(b) Braunschweig velocity profile

Fig. 2: Standard velocity profiles used in this work.

$$\omega_{ice,k} = \frac{\delta_{g,k} i_f}{r_w} v_{veh,k} \vartheta_k, \quad (10)$$

and $\vartheta_k \in \{0,1\}$ is the binary variable representing the switching start/stop of the ICE, where 1 indicates the engine is on and 0 indicates that the engine is off.

The force experienced by the wheels and required to overcome all resistance forces is depending on the parallel hybrid configuration as:

$$F_{w,k} = \begin{cases} \frac{\delta_{g,k} i_f}{r_w}(u_{ice,k} + u_{em,k})\vartheta_k & \text{if P0 or P1} \\ \frac{\delta_{g,k} i_f}{r_w}(u_{ice,k}\vartheta_k + u_{em,k}) & \text{if P2} \\ \frac{1}{r_w}(u_{ice,k}\vartheta_k \delta_{g,k} i_f + u_{em,k}) & \text{if P3 or P4} \end{cases}, \quad (11)$$

where the configuration $P0$ and $P1$ represent the EM connected to the ICE by a belt and the start/stop system affects both components. Configuration $P2$ represents the EM being positioned in the shaft before the transmission. The $P3$ and $P4$ configuration represents the configuration where the EM is connected directly to the shaft after the transmission via a gear mesh. This

work focuses on a pre-transmission (P2) parallel hybrid configuration, where the EM is mounted to the same shaft as the ICE before entering the gearbox [18], therefore introducing the HEV configuration (11) and resistance forces (7), (8) and (9), into (6) yields:

$$u_{ice,k}\vartheta_k + u_{em,k} - u_{br,k} = T_{req,k}, \tag{12}$$

where $T_{req,k}$ represents the torque required to move the vehicle and is obtained by:

$$T_{req,k} = \frac{r_w}{\delta_{g,k} i_f}\left(I_{veh,k}\frac{v_{veh,k+1}-v_{veh,k}}{\Delta_t} + F_{r,k} + F_{d,k}\right), \tag{13}$$

moreover, the torque provided by the ICE is bounded by:

$$\underline{u}_{ice} \leq u_{ice,k} \leq \overline{u}_{em}. \tag{14}$$

D. Electric motor

The EM is modeled as a power converter, describing the relationship and efficiency between electrical power y_{em}, torque u_{em} and angular speed ω_{em},

$$y_{em,k} = \gamma_3 u_{em,k}^2 + \gamma_2 \omega_{em,k} u_{em,k} + \gamma_1 \omega_{em,k}, \tag{15}$$

where γ_i, $i \in \{1,2,3\}$ are polynomial coefficients, and similarly as for the ICE fuel rate consumption model, are obtained through least squares:

$$\min_{\Psi_{em}} ||e_{em}||_2^2 = ||Y_{em} - W_{em}\Psi_{em}||_2^2, \tag{16}$$

where Ψ_{em} corresponds to:

$$\Psi_{em} = [\gamma_3, \gamma_2, \gamma_1]^\top, \tag{17}$$

Y_{em} and W_{em} are the power, angular speed and torque evolution of the EM as:

$$Y_{em} = \begin{bmatrix} y_{em,1} \\ y_{em,2} \\ \vdots \\ y_{em,N} \end{bmatrix}, \quad W_{em} = \begin{bmatrix} u_{em,1}^2 & \omega_{em,1}u_{em,1} & \omega_{em,1} \\ u_{em,2}^2 & \omega_{em,2}u_{em,2} & \omega_{em,2} \\ \vdots & \vdots & \vdots \\ u_{em,N}^2 & \omega_{em,N}u_{em,N} & \omega_{em,N} \end{bmatrix}, \tag{18}$$

and the coefficient as well as mean square error can be found in Table I. Similar to the torque the ICE can provide, the EM torque is bounded by:

$$\underline{u}_{em} \leq u_{em,k} \leq \overline{u}_{em}, \tag{19}$$

and the angular speed of EM is given by:

$$\omega_{em,k} = \frac{\delta_{g,k} i_f}{r_w} v_{veh}. \tag{20}$$

Furthermore, for the case study at hand, the considered vehicle is a rear-wheel driven, and is assumed that only 50% of the negative torque provided by the velocity profile can be met by the EM regenerative braking and the remaining 50% is assumed to be provided by the mechanical brakes.

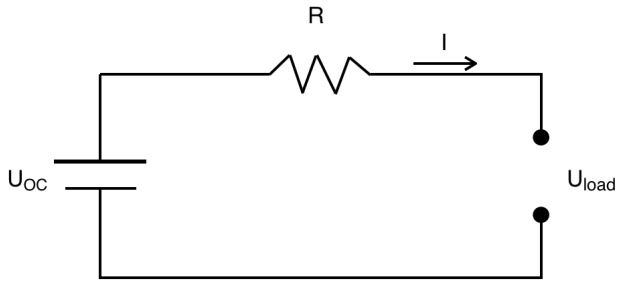

Fig. 3: Battery equivalent circuit

E. High voltage battery subsystem

The vehicle is equipped with a battery which supplies power according to the demand from the driveline EM. The battery system can be represented by an equivalent circuit model which contains a voltage source with a constant open circuit voltage U_{oc} in series with a resistance R. Its voltage is governed by Kirchhofs law:

$$U_{oc} = I_k R + U_{load,k}. \tag{21}$$

From (21) the power converter describing the efficiency of the subsystem can be re-written taking the battery output power as $y_{hvb,k} = U_{load,k} I_k$ and the battery input power as $u_{hvb,k} = U_{oc} I_k$, yielding:

$$y_{hvb,k} = \beta u_{hvb,k}^2 + u_{hvb,k}, \tag{22}$$

where $\beta = -\frac{R}{U_{oc}^2}$ and the values for R and U_{oc} of the case study can be found in Table I.

The discrete-time battery stored charge dynamics, can be approximated to its relation with current as:

$$x_{k+1} = x_k - \Delta_t u_{hvb,k}, \tag{23}$$

where x_k represents the charge of the battery at time k. Having positive current means that the battery is supplying energy to the network and negative current means the battery is charging, and where both the HVB energy and power are bounded for all times by:

$$\underline{x} \leq x_k \leq \overline{x} \tag{24a}$$

$$\underline{u}_{hvb} \leq u_{hvb,k} \leq \overline{u}_{hvb}. \tag{24b}$$

F. Braking

The mechanical brake functions as a load balancing and torque excess dissipation. This subsystem does not store energy making it a terminal subsystem, where only positive breaking torque is possible, i.e.,

$$u_{br} \geq 0. \tag{25}$$

G. Optimal Control Problem Formulation

The goal for this project is to minimize the cumulative fuel consumption (1) given by the fuel rate expression (2), while in the presence of integer decision variables $\vartheta_k \in \{0,1\}$. Obtaining the torque split between ICE and EM (12) in order to reach a known velocity profile, and respecting the power flow interaction between EM and HVB (15), (22), (23).

Therefore the Optimal Control Problem is written as:

$$\min_{u_{m,k},x_k,\vartheta_k} \sum_{k\in\mathscr{K}} m_{f,k}\cdot\vartheta_k \tag{26a}$$

subject to:

$$m_{f,k} = \alpha_1\omega_{ice,k} + \alpha_2\omega_{ice,k}^2 + \alpha_3\omega_{ice,k}u_{ice,k} \tag{26b}$$

$$y_{hvb,k} = \beta u_{hvb,k}^2 + u_{hvb,k} \tag{26c}$$

$$y_{em,k} = \gamma_3 u_{em,k}^2 + \gamma_2\omega_{em,k}u_{em,k} + \gamma_1\omega_{em,k} \tag{26d}$$

$$u_{ice,k}\cdot\vartheta_k + u_{em,k} - u_{br,k} - T_{req,k} = 0 \tag{26e}$$

$$y_{hvb,k} = y_{em,k} \tag{26f}$$

$$x_{k+1} = x_k + \Delta_t u_{hvb,k} \tag{26g}$$

$$u_{m,k} \in [\underline{u}_m, \overline{u}_m] \tag{26h}$$

$$x_k \in [\underline{x}, \overline{x}] \tag{26i}$$

$$\vartheta_k \in \{0,1\}, \tag{26j}$$

where $m \in \mathscr{M} = \{ice, em, hvb, br\}$.

The above mentioned problem falls in the category of Mixed-Integer Nonlinear Program (MINLP). Due to the nature of the start/stop variable, the nonlinearity caused by the product of the ICE torque with the start/stop variable and the quadratic relationship in the converters.

III. Solution approaches

In this section three methodologies in order to handle the binary variable are going to be introduced. Moreover, these methodologies are applied to the previously MINLP presented in the last section in order to compare complexity in problem formulation, minimization time and resulting fuel consumption.

The three approaches in order to handle the binary variable considered in this work are:

a) Firstly, a trajectory of ϑ_k for all times $\mathscr{K}$ is given (as similarly done in [13]), simplifying the problem (26) because the dependency of the integer variable no longer exists, the OCP only depends on continuous variables. This simplification affects the objective function (26a) and torque split (26e) making them both linear. As a consequence, the original MINLP becomes a Quadratically Constrained Linear Program (QCLP). In this work, the CPLEX solver developed by IBM [19] is used to solve the QCLP.

b) A second approach, is to make an outer relaxation $\vartheta_k \in \{0,1\}$ to $\vartheta_k \in [0,1]$. It can now take any value between 0 and 1, as in [14]. This relaxation directly affects the objective function (26a) and the torque split (26e) and the dependency on the binary variable disappears. Hence, the original MINLP becomes a nonlinear program (NLP). This NLP can be solved by a Sequential Quadratic Programming (SQP) algorithm as in [10], in which the nonlinear objective function and constraints are approximated by quadratic and linear functions, respectively. This yields a sequence of new quadratic programs. After the SQP has converged, the binary variable can be recovered by rounding the solution of the continuous relaxed ϑ, and can be fed into the above mentioned approach (a)) as given sequence $\{\vartheta_1, \ldots \vartheta_{K-1}\}$.

c) Lastly, in our third approach, we approximate the nonlinear objective function and constraints by sequentially formulating quadratic and linear functions as done in b), while maintaining $\vartheta_k \in \{0,1\}$. This approach is referred as Sequential Mixed-Integer Quadratic Programing (S-MIQP) [16]. The sequence of new Mixed-Integer Quadratic Programs (MIQP) are then fed into a dedicated commercial solver which can handle binary variables. In this work, CPLEX is used in order to handle the binary variables.

A. Quadratically Constrained Linear Program

As mentioned in the introduction of this section, the first approach taken is to have a known trajectory of the start/stop variable. In order to obtain an upper bound of the fuel consumption solution, we assume:

$$\vartheta_k = 1 \quad \forall k \in \mathscr{K}. \tag{27}$$

It can be seen from (26a) and (26b) that even if there is no torque provided by the ICE, due to the angular speed of the combustion engine and $\vartheta = 1$ for all times, there will be fuel consumption. This assumption is taken in order to compare fuel consumption savings with the following approaches where ϑ is allowed to switch.

This assumption yields a new OCP which is linear in its objective function and is quadratically constrained by the power balance equation of the power node, and linearly constrained by the torque balance and battery dynamics respectively. Therefore the reformulated

QCLP OCP becomes:

$$\min_{u_{m,k},x_k} \sum_{k\in\mathscr{K}} (\alpha_1 \omega_{ice,k} + \alpha_2 \omega_{ice,k}^2 + \alpha_{3,} \omega_{ice,k} u_{ice,k}) \tag{28a}$$

subject to:

$$y_{hvb,k} = \beta u_{hvb,k}^2 + u_{hvb,k} \tag{28b}$$
$$y_{em,k} = \gamma_3 u_{em,k}^2 + \gamma_2 \omega_{em,k} u_{em,k} + \gamma_1 \omega_{em,k} \tag{28c}$$
$$u_{ice,k} + u_{em,k} - u_{br,k} = T_{req,k} \tag{28d}$$
$$y_{hvb} = y_{em} \tag{28e}$$
$$x_{k+1} = x_k + \Delta_t u_{hvb,k} \tag{28f}$$
$$u_{m,k} \in [\underline{u}_m, \overline{u}_m] \tag{28g}$$
$$x_k \in [\underline{x}, \overline{x}]. \tag{28h}$$

The result of this minimization yields an upper bound to our original MINLP problem (26), meaning that solutions found when taking the variable ϑ_k as switching variable, will always yield lower fuel consumption.

B. Outer approximation and Sequential Quadratic Programming

A second approach to solve (26) is by relaxing (26j) so that $\vartheta_k \in [0,1]$, yielding a new NLP. This NLP is solved through Sequential Quadratic Programming, but can be solved through any commercial solvers that can handle nonlinearities in objective function and constraints. The obtained NLP is of the form:

$$\min_{u_{m,k},x_k,\vartheta_k} \sum_{k\in\mathscr{K}} \alpha_1 \omega_{ice,k} \vartheta_k + \alpha_2 \omega_{ice,k}^2 \vartheta_k + \alpha_3 \omega_{ice,k} u_{ice,k} \vartheta_k \tag{29a}$$

subject to:

$$y_{hvb,k} = \beta u_{hvb,k}^2 + u_{hvb,k} \tag{29b}$$
$$y_{em,k} = \gamma_3 u_{em,k}^2 + \gamma_2 \omega_{em,k} u_{em,k} + \gamma_1 \omega_{em,k} \tag{29c}$$
$$u_{ice,k} \vartheta_k + u_{em,k} - u_{br,k} = T_{req,k} \tag{29d}$$
$$y_{hvb,k} = y_{em,k} \tag{29e}$$
$$x_{k+1} = x_k + \Delta_t u_{hvb,k} \tag{29f}$$
$$u_{m,k} \in [\underline{u}_m, \overline{u}_m] \tag{29g}$$
$$x_k \in [\underline{x}, \overline{x}] \tag{29h}$$
$$\vartheta_k \in [\underline{\vartheta}, \overline{\vartheta}]. \tag{29i}$$

From problem (29), it can be seen that (29a), (29d), (29b) and (29c) are non-linear in decision variables. In order to obtain a solution, a Sequential Quadratic Program (SQP) is implemented. SQP aims at solving a nonlinear optimal control problem by sequentially solving Quadratic Programs (QP's) which are constructed by quadratically approximating the objective function and linearizing constraints.

The implemented SQP algorithm to obtain a solution of (29) is:

$$\underset{z_k}{\operatorname{argmin}} \ \textstyle\sum_{k\in\mathscr{K}} \frac{1}{2} \left(z_k - z_k^i\right)^\top R_k \left(z_k - z_k^i\right) + \left(H_k z_k^i + F_k\right)^\top z_k \tag{30a}$$

subject to:

$$\tilde{T}_{b,k} = 0 \tag{30b}$$
$$\tilde{y}_{hvb,k} - \tilde{y}_{em,k} = 0 \tag{30c}$$
$$x_{k+1} = x_{hvb,k} + \Delta_t u_{hvb,k} \tag{30d}$$
$$u_{m,k} \in [\underline{u}_m, \overline{u}_m] \tag{30e}$$
$$x_k \in [\underline{x}, \overline{x}] \tag{30f}$$
$$\vartheta_k \in [\underline{\vartheta}, \overline{\vartheta}], \tag{30g}$$

where H_k and F_k represent the Hessian and Gradient of (29a):

$$H_k = \begin{bmatrix} 0 & 0 & 0 & 0 & 0 & \frac{1}{2}\alpha_3 \omega_{ice,k} \\ 0 & 0 & 0 & 0 & 0 & 0 \\ 0 & 0 & 0 & 0 & 0 & 0 \\ 0 & 0 & 0 & 0 & 0 & 0 \\ 0 & 0 & 0 & 0 & 0 & 0 \\ \frac{1}{2}\alpha_3 \omega_{ice,k} & 0 & 0 & 0 & 0 & 0 \end{bmatrix}, \tag{31}$$

$$F_k = [0,0,0,0,0,\alpha_1 \omega_{ice,k} + \alpha_2 \omega_{ice,k}^2], \tag{32}$$

and $R_k \succeq 0$ ensures that the objective function is convex. Furthermore, we propose to generate a quadratic approximation of the objective function around $(z^i)^\top$, i.e.,

$$\frac{1}{2} \left(z_k - z_k^i\right)^\top R_k \left(z_k - z_k^i\right) + \left(H_k z_k^i + F_k\right)^\top z_k, \tag{33}$$

where for compactness of notation the decision variables are grouped as:

$$z_k^i = [u_{ice,k}^i, u_{em,k}^i, x_k^i, u_{hvb,k}^i, \vartheta_k^i, u_{br,k}^i], \tag{34}$$

for all $k \in \mathscr{K}$, i representing the iteration number of the SQP algorithm. Also for the torque balance, EM and HVB converters, a linear approximation around point $(z_k^i)^\top$ is performed i.e.,

$$\tilde{T}_{b,k} = T_{b,k}^i + \nabla_z T_{b,k} \left(z_k - z_k^i\right), \tag{35}$$
$$\tilde{y}_{em,k} = y_{em,k}^i + \nabla_z y_{em,k} \left(z_k - z_k^i\right), \tag{36}$$
$$\tilde{y}_{hvb} = y_{hvb,k}^i + \nabla_z y_{hvb,k} \left(z_k - z_k^i\right), \tag{37}$$

where $T_{b,k}$ represents the torque balance given by:

$$T_{b,k}^i = u_{ice,k}^i \vartheta_k^i + u_{em,k}^i - u_{br,k}^i + T_{req,k}. \tag{38}$$

Equation (30) is solved for all $k \in \mathscr{K}$ and $i \in \mathbb{N}$, starting the algorithm with a chosen $\{z_k^0\}$ such that a feasible solution exists for the next iteration of SQP. The SQP algorithm can be terminated by reaching a

predefined maximum number of SQP iterations or once the difference in cost of the new recovered solution and the previous solution reaches a certain tolerance as:

$$|J^{i+1} - J^i| \leq \Delta_{tol}, \tag{39}$$

where J^i is (30a) evaluated at iteration i.

Solving the MINLP by relaxing ϑ to be continuous and solving the resulting NLP yields a lower bound to the solution of original MINLP problem. Rounding the continuous solution of ϑ can be done in order to obtain a binary trajectory. Given that the torque the EM can provide is bounded by (19), rounding off the obtained continuous solution of (29) may lead to infeasibility, therefore an intermediate step has to be taken. Once the trajectory of the start/stop variable is known and rounded, it can be fed as known information to the QCLP (28) described in Section III-A, in order to find a feasible trajectory for the EM torque and its corresponding HVB energy.

C. Sequential Mixed-Integer Quadratic Programming

A third approach towards solving (26), is to implement a Sequential Mixed Integer Quadratic Programming (S-MIQP) as done in [16]. Similarly to III-B, a quadratic approximation for the objective function (26a), linear approximation of non-linear constraints (26e), (26c) and (26d) is done, yielding a new Mixed-Integer Quadratic Program:

$$\underset{z_k}{\operatorname{argmin}} \ \sum_{k\in\mathscr{K}} \tfrac{1}{2}\left(z_k - z_k^i\right)^\top R_k \left(z_k - z_k^i\right) + \left(H_k z_k^i + F_k\right)^\top z_k \tag{40a}$$

subject to:

$$\tilde{T}_{b,k} = 0 \tag{40b}$$
$$\tilde{y}_{hvb,k} - \tilde{y}_{em,k} = 0 \tag{40c}$$
$$x_{k+1} = x_k + \Delta_t u_{hvb,k} \tag{40d}$$
$$u_{m,k} \in [\underline{u}_m, \overline{u}_m] \tag{40e}$$
$$x_k \in [\underline{x}, \overline{x}] \tag{40f}$$
$$\vartheta_k \in \{\underline{\vartheta}, \overline{\vartheta}\}. \tag{40g}$$

Where R_k is chosen such that (40a) is convex, and $\{z_k^0\}_{k\in\mathscr{K}}$ chosen such that a feasible solution exists for the next iteration.

IV. Results

In this section the obtained results are presented. First, subsection IV-A gives a series of steps in order to reduce the number of decision variables and complexity of the OCP's presented. Finally, numerical results of the minimization times and fuel consumed are shown in subsection IV-B.

A. Implementation

In order to reduce the number of decision variables and the complexity of the above presented problems, several steps are taken. First, the information contained in the equality describing the fuel rate consumption (26b) is brought into the objective function (26a) by substitution [20]. Second, the quadratic equality constraints representing the efficiency of the HVB and EM converters (26c), (26d) are substituted into the equality constraint describing their interaction in the power node (26f), which, for the case presented in III-A, is turned into an inequality constraint to reach a convex OCP. Third, given that the braking torque ($u_{br,k}$) can only take positive values (25), the torque balance equation can be reformulated as an inequality constraint:

$$u_{ice,k}\vartheta_k + u_{em,k} \leq T_{req,k}, \tag{41}$$

and can be recovered once the solution is obtained. Furthermore, the dynamics of the battery described by (26g) can be recasted as a prediction model:

$$\mathscr{X} = \Phi_{hvb} x_0 + \Gamma_{hvb}\mathscr{U}_{hvb}, \tag{42}$$

where

$$\Phi_{hvb} = \begin{bmatrix} 1 & 1 & \dots & 1 \end{bmatrix}^\top, \qquad \Gamma_{hvb} = \begin{bmatrix} \Delta_t & 0 & \dots & 0 \\ \Delta_t & \Delta_t & \dots & 0 \\ \vdots & \vdots & \ddots & \vdots \\ \Delta_t & \Delta_t & \dots & \Delta_t \end{bmatrix}, \tag{43}$$

equation (42) is bounded for all times by (24a) and can now enter as linear inequality constraints.

B. Simulation results

For the case study at hand, two velocity profiles are considered. The New York City Cycle (NYCC), simulating low speed city driving and Braunschweig, simulating urban route with higher velocities. This profiles can be seen in Figure 2a and 2b. For both profiles, five cases are considered:

I ICE only vehicle.
II HEV with $\vartheta = 1$ (upper bound).
III HEV with outer approximation $\vartheta \in [0,1]$ (lower bound).

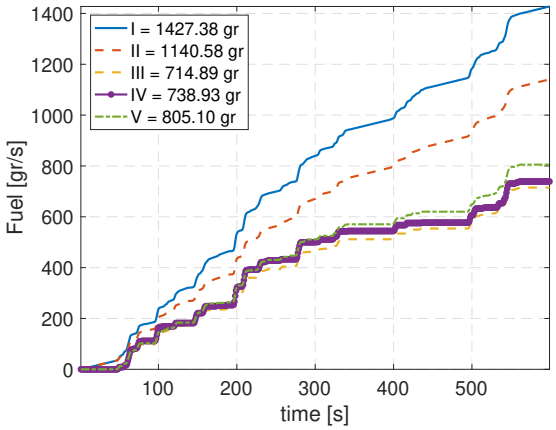

(a) NYCC velocity profile.

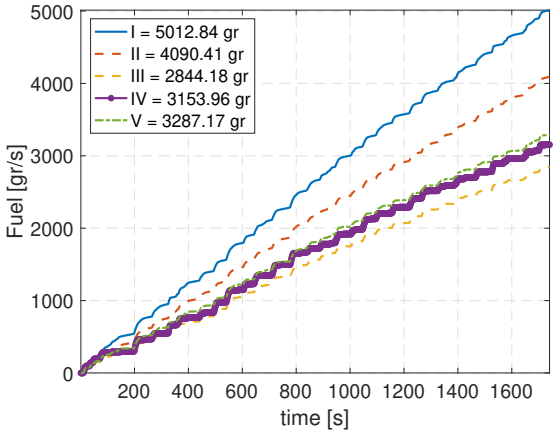

(b) Braunschweig velocity profile.

Fig. 4: Cumulative fuel consumption NYCC and Braunschweig profiles

IV HEV with outer approximation and rounding.
V HEV with S-MIQP.

From Figure 4 can be seen how cases I and II are constantly increasing in their fuel consumption. This is because even when the combustion engine is not providing torque, the system keeps on consuming fuel. On the other hand, cases III, IV, and V clearly show the engine shuts Off in several points along the trajectories. It is noticeable for both profiles how case II yields the highest fuel consumption (for the HEV cases) due to the assumption that for all times the ICE is kept ON, and how III has the lower fuel consumption, this due to the relaxation of the binary variable in order to take any values between 0 and 1. Even though case III is not an implementable solution, it serves for benchmarking purposes.

Due to the engine switching, fuel consumption reductions of 35.2% between case IV and II, and reductions of 29.4% between V and II)for the NYYC profile are found. In addition, for the Braunschweig profile, the reductions are of 22.8% and 19.6%, respectively.

The corresponding fuel consumed and minimization time taken for each case are found in Table II. Analyzing the minimization time results, it can be concluded that if the minimization time is critical and the trajectory of the binary variable is known, case II should be implemented. However, if the start/stop variable is unknown, case IV or case V should be used in order to obtain it with the rest of the decision variables. From these two cases, case V is the faster with lower minimization time compared to IV (98% faster in NYCC profile), although this minimization time difference shortens considerably for longer horizons as seen for the Braunschweig profile (38% faster). If the minimization time is not critical, and the fuel consumption is seeked to be lower, case IV yields better results than case V (4% lower for the NYYC profile and 8% lower for Braunschweig).

Finally, Figure 5 and 6 presents the behaviour of the start/stop variable obtained from the relaxed solution (case III), rounded solution (case IV) and binary solution (case V). It can be seen how the recovered solution from case III contains values between 0 and 1 in several moments of the horizon, and how the rounding solution (case IV) affects the variable. Furthermore, case V presents more instances where the ICE is ON which explains the higher fuel consumption in both profiles presented in Table II.

TABLE II: Fuel consumption and minimization time taken for each case in both profiles.

Case	NYCC		Braunschweig	
	Fuel [gr]	Min time [s]	Fuel [gr]	Min time [s]
I	1427.38	0.15	5012	0.15
II	1140.58	3.6	4091.41	51.28
III	714.89	35787.47	2844.18	19716.61
IV	738.93	35793.83	3153.96	19832.67
V	805.1	704.4	3287.17	12286.29

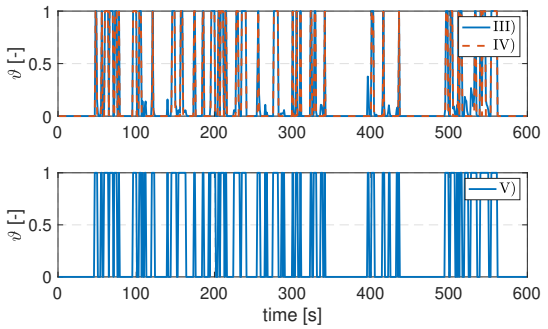

(a) Continuous, rounded and binary ϑ solutions for NYCC profile.

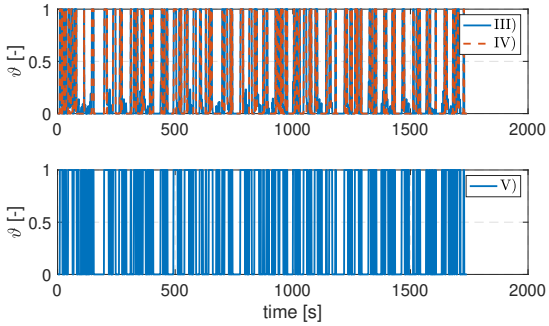

(b) Continuous, rounded and binary ϑ solutions for Braunschweig profile.

Fig. 5: Cases III, IV and V solution for both NYCC and Braunschweig profiles.

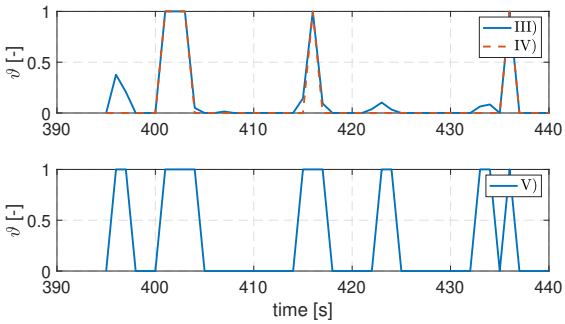

(a) Continuous, rounded and binary ϑ solutions for NYCC profile.

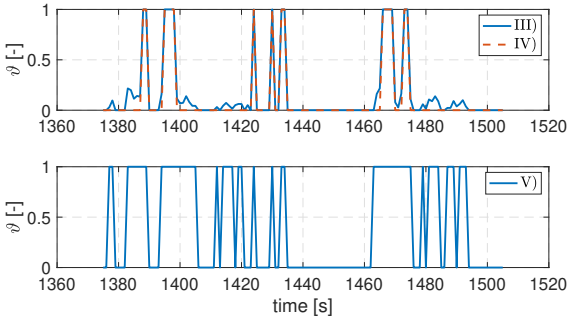

(b) Continuous, rounded and binary ϑ solutions for Braunschweig profile.

Fig. 6: Inset for NYCC and Braunschweig profiles of ϑ solutions.

V. Conclusion

In this thesis we have presented an Optimal Control Problem (OCP) formulation describing the Vehicle Energy Management (VEM) problem for a hybrid electric heavy duty truck which includes engine start/stop. We have formulated it as a Mixed-Integer Nonlinear Program static optimization problem and presented three methodologies in order to handle the binary start/stop decision variable. In the first approach, the start/stop variable is assumed to be On through out all time yielding an upper bound for the fuel consumption solution. Second, doing a relaxation of the binary variable and taking it as continuous, finding a lower bound of solution to the original problem and recovering the binary variable by rounding. Finally, doing sequential mixed-integer quadratic program approximation of the original problem.

In future work, subsystems such as heating ventilation and air conditioning (HVAC) and more auxilaries could be added to the network topology, which can be solved by Complete Vehicle Energy Management (CVEM), in order to see the difference in solution and computational time. Finally, another open path to exploration is solving the original MINLP problem by implementing genetic algorithms and benchmarking the solution in terms of time and solution accuracy against dynamic programming.

References

[1] "Intergovernmental panel on climate change," *Climate change 2014: mitigation of climate change, volume 3*, Cambridge University Press, 2015.

[2] D. P. Bertsekas, "Dynamic programming and optimal control," *Athena Scientific, Vol I*, 2005.

[3] J. Liu and H. Peng, "Modeling and control of a power-split hybrid vehicle," *IEEE Transactions on Control Systems Technology, Vol. 16, No. 6*, 2008.

[4] Z. Yuan, L. Teng, S. Fengchun, and H. Peng, "Comparative study of dynamic programming and pontryagin's minimum principle on energy management for a parallel hybrid electric vehicle," *Energies, vol. 6, no. 4*, 2013.

[5] R. Wang and S. M. Lukic, "Dynamic programming technique in hybrid electric vehicle optimization," *IEEE International Electric Vehicle Conference*, 2012.

[6] Y. Chamaillard, G. Colin, K. Gillet, D. Maamria, and C. Nouillant, "Computation of eco-driving cycles for hybrid electric vehicles: Comparative analysis," *Control Engineering Practice*, 2018.

[7] F. Merz, A. Sciarreta, J. Dabadie, and L. Serrao, "On the optimal thermal management of hybrid-electric vehicles with

heat recovery system." *Oil and Gas Science and Technology*, 2012.
[8] R. F. Hartl, S. P. Sethi, and R. G. Vickson, "A survey of the maximum principles for optimal control problems with state constraints," *SIAM Rev., vol. 27*, 1995.
[9] M. Sánchez, S. Delprat, and T. Hofman, "Energy management of hybrid vehicles with state constraints: A penalty and implicit hamiltonian minimization approach," *Applied Energy*, 2020.
[10] Z. Khalik, G. Padilla, T. Romijn, and M. Donkers, "Vehicle energy management with ecodriving: A sequential quadratic programming approach with dual decomposition," *Annual American Control Conference, ACC*, 2018.
[11] T. Romijn, M. Donkers, J. Kessels, and S. Weiland, "A distributed optimization approach to complete vehicle energy management," *IEEE Trans Control Syst Technol*, 2018.
[12] R. Vadamalu and C. Beidl, "Online optimization based energy management of hybrid electric vehicles using direct optimal control." *Internationales Stuttgarter Symposium*, 2016.
[13] K. Elands, "Mode switching control with preview information for a multimodal heavy-duty hybrid powertrain," Technische Universiteit Eindhoven, MSc. thesis 2019.
[14] Y. Chen and M. Lazar, "On real-time driver advice system design for predictive eco-driving," *IFAC World Congress*, 2020.
[15] A. Fröberg and L. Nielsen, "Optimal fuel and gear ratio control for heavy trucks with piece wise affine engine characteristics," *Advances in Automotive Control*, 2007.
[16] C. Pelosi, G. Padilla, and M. Donkers, "Energy optimal coordination of fully autonomous vehicles in urban intersections," *IFAC World Congress*, 2019.
[17] B. Saerens, "Optimal control based eco-driving," Katholieke Universiteit Leuven, PhD thesis 2012.
[18] L. Guzzella and A. Sciarretta, *Vehicle propulsion systems: Introduction to modeling and optimization*, 01 2007.
[19] IBMCorporation, "Ibm ilog cplex optimization studio," 2019.
[20] S. Boyd and L. Vandenberghe, "Convex optimization," Cambridge University Press, 2019.

APPENDIX I: GEAR SELECTION ALGORITHM

Algorithm 1 The gear shifting strategy in this algorithm is used in II-B.

Input: Horizon $K \in \mathbb{N}$, velocity profile $v_{veh,k} \forall k \in \mathbb{N}$.
Output: $\delta_{g,k} \forall k \in \mathbb{N}$, $a_{veh,k} \forall k \in \mathbb{N}$.
Define v_{up} {%Shift up velocity threshold}
Define v_{down} {%Shift down velocity threshold}
Define gears {%Vector containing number of gears in gearbox}
Define ratio {%Vector containing the ratios according to each gear in the gearbox}
Define maxGear = max(gears) {%Highest possible gear}
Define minGear = min(gears) {%Lowest possible gear}
$a_{veh} \leftarrow diff(\mathrm{v}_{veh})$ {%Compute acceleration}
for k = 1 to N **do**
  if $a_{veh,k} > 0$ **then**
    I_{up} = find($v_{up} \geq v_{veh,k}$)
    Sel = min(I_{up})
    if Sel = NaN **then**
      Sel = maxGear
    end if
    $\delta_{g,k}$ = ratio(sel)
  end if
  if $a_{veh,k} < 0$ **then**
    I_{down} = find($v_{down} \leq v_{veh,k}$)
    Sel = max(I_{down})
    if Sel = NaN **then**
      Sel = minGear
    end if
    $\delta_{g,k}$ = ratio(Sel)
  end if
  if $a_{veh,k} = 0$ and $v_{veh,k} > 0$ **then**
    $\delta_{g,k} = \delta_{g,k-1}$
  end if
  if $a_{veh,k} = 0$ and $v_{veh,k} = 0$ **then**
    $\delta_{g,k}$ = minGear
  end if
end for